Strong Gravitational Lensing in the Era of Big Data
Proceedings IAU Symposium No. 381, 2024
H. Stacey, A. Sonnenfeld & C. Grillo, eds.
doi:10.1017/S1743921323004039

Shapes and Centroids of 39 Strong Lensing Galaxy Clusters from the Sloan Giant Arcs Survey

Raven Gassis[1], Matthew B. Bayliss[1], Keren Sharon[2], Guillaume Mahler[3], Michael D. Gladders[4], Håkon Dahle[5], Michael K. Florian[6], Jane R. Rigby[7], Lauren Elicker[1] and M. Riley Owens [1]

[1]Department of Physics, University of Cincinnati. email: gassismr@mail.uc.edu

[2]Department of Astronomy, University of Michigan,

[3]Centre for Extragalactic Astronomy, Durham University,

[4]Department of Astronomy and Astrophysics/Kavli Institute for Cosmological Physics, University of Chicago,

[5]Institute of Theoretical Astrophysics, University of Oslo,

[6]Steward Observatory,

[7]University of Arizona, Observational Cosmology Lab, Code 665, NASA Goddard Space Flight Center

Abstract. Strong lensing galaxy clusters provide a powerful observational test of Cold Dark Matter (CDM) structure predictions derived from simulation. Specifically, the shape and relative alignments of the dark matter halo, stars, and hot intracluster gas tells us the extent to which theoretical structure predictions hold for clusters in various dynamical states. We measure the position angles, ellipticities, and locations/centroids of the brightest cluster galaxy (BCG), intracluster light (ICL), the hot intracluster medium (ICM), and the core lensing mass for a sample of strong lensing galaxy clusters from the SDSS Giant Arcs Survey (SGAS). We use iterative elliptical isophote fitting methods and GALFIT modeling on HST WFC3/IR imaging data to extract ICL and BCG information and use `CIAO's Sherpa` modeling on Chandra ACIS-I X-ray data to make measurements of the ICM. Using this multicomponent approach, we attempt to constrain the physical state of these strong lensing clusters and evaluate the different observable components in terms of their ability to trace out the gravitational potential of the cluster.

Keywords. Strong Lensing Galaxy Clusters (SLGCs), Brightest Cluster Galaxy (BCG), Intracluster Medium (ICM), Intracluster Light (ICL)

1. Introduction

An important consequence of Λ Cold Dark Matter (ΛCDM) physics is that galaxy clusters form by the hierarchical formation of DM halo systems. In this scenario, the cluster gradually accretes and incorporates other haloes, eventually forming one large mass halo system that defines the cluster (Beers and Geller 1983).

In a theoretical system only subject to gravitational forces, the brightest cluster galaxy (BCG), intracluster light (ICL), and the hot intracluster medium (ICM) of a given galaxy cluster should align with the dark matter halo of the cluster defined by the core lensing

mass (Sastry 1968; Binggeli 1982; Van Den Bosch et al. 2005; Hashimoto et al. 2008; Niederste-Ostholt et al. 2010; Biernacka et al. 2015; Donahue et al. 2016; Wang et al. 2018).

Though there is broad agreement with the predicted alignment, previous work has found that some of the mass components are not always aligned with the dark matter halo or with each other (Van Den Bosch et al. 2005; Sanderson et al. 2009; Skibba et al. 2011; Zitrin et al. 2012; Hikage et al. 2013; Lauer et al. 2014; Martel et al. 2014; Oliva-Altamirano et al. 2014; Wang et al. 2014; Hoshino et al. 2015; Rossetti et al. 2016; Lange et al. 2018; Lopes et al. 2018; Zenteno et al. 2020; De Propris et al. 2021). This suggests that there are mechanisms by which misalignments can occur in the context of ΛCDM or potentially beyond ΛCDM.

Given enough time to relax, the BCG and ICL should revert to their shared orientation and centroid with their dark matter halo (Montes and Trujillo 2018; Wittman et al. 2019). However, work by Kim et al. (2017) and Harvey et al. (2017) found that the BCG can still show misalignments ("wobble") in relaxed clusters which is unaccounted for in the cold dark matter description. Though the ICL is not expected to have any residual "wobbling", DM measurements derived from strong lensing mass models allow us to directly test whether the ICL traces out the shape of the DM halo as predicted.

The ICM gas can exhibit extreme misalignments for disturbed clusters due to merger activity. Even for relaxed clusters, hydrodynamical gas oscillations can cause some deviations in the ICM to persist even when the other components of the cluster system have had time to relax (Markevitch et al. 2001; Churazov et al. 2003; Johnson et al. 2012; Harvey et al. 2017).

2. Data and Measurements

In this work, we apply a multicomponent observational approach incorporating measurements of the BCG, ICL, ICM, and core lensing mass derived from strong lensing. We investigate 39 clusters from the Sloan Giant Arcs Survey (SGAS) with corresponding multiband *HST* data and spectroscopic follow up that enabled well constrained strong gravitational lensing models (Sharon et al. 2020, 2022a,b). A subset of 27 clusters have *Chandra* observations that allow us to make measurements on the BCG, ICL, ICM, and core lensing mass simultaneously.

2.1. *BCG/ICL Measurement*

We modeled the BCG using GALFIT in order to eliminate all interfering light. For the ICL, we derived masks for all objects in the field using `SExtractor`. For both the ICL and BCG, we use iterative elliptical isophote fitting applying the Python `lsq-ellipse` function. To differentiate between the BCG and ICL, we conduct a radial profile analysis of our clusters to find the ICL/BCG transition radius to be about 50 kpc which is consistent with 60 ± 40 kpc as measured by Contini et al. (2022).

2.2. *ICM Measurement*

For the ICM gas, we use the publicly available `CIAO` tools for data reduction to process the Chandra X-ray event data. Each processed X-ray image file was point source subtracted, binned by 2", and set to only include events in the broad energy band (0.5-7 keV with an effective energy of 2.3 keV). We modeled the processed ICM distribution using `CIAO's Sherpa` modeling functions and took the outputted best fit as the true parameters.

https://doi.org/10.1017/S1743921323004039 Published online by Cambridge University Press

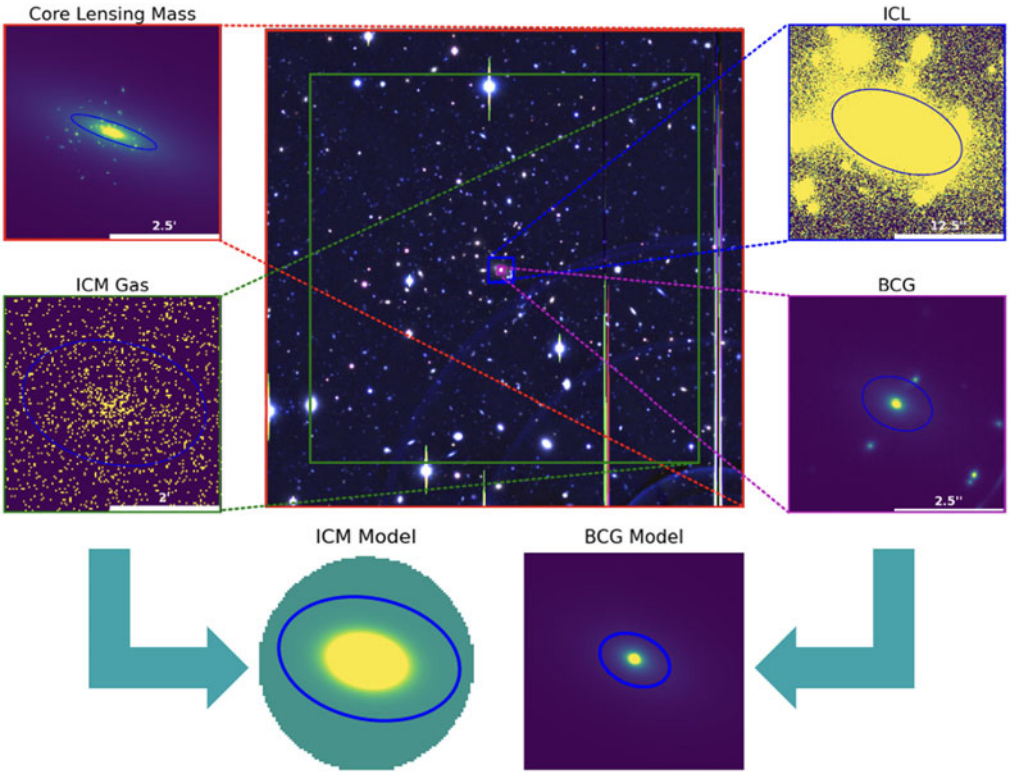

Figure 1. Visualization of the data distributions with the corresponding best fit ellipse for example galaxy cluster J0957p0509. We include a 5"x5" representative color (gri) Subaru image of the field in the center panel for a scale comparison of the different distributions. The ICM and BCG also have visualizations of their models that precede ellipse fitting.

2.3. *Strong Lensing Models and Core Lensing Mass Measurement*

The strong lensing models for these galaxy clusters were derived using the publicly available Lenstool software (Jullo et al. 2007). The lensing models are more fully described in Sharon et al. 2020, 2022a,b. We use 100 lens models drawn from the `Lenstool` MCMC with the derived lensing parameters to sample the posterior probability distribution. In the image plane models, there is an obvious core cluster that dominates the distribution at large scales. This is the core mass distribution we would expect to align with the BCG, ICL, and ICM components. We choose the core lensing mass parameters from the most likely image plane model to be the true values.

3. Results

3.1. *Position Angles*

Figure 2 shows the results of the various cluster components' position angles compared to the position angle of the core lensing mass. Equation 1 defines the difference in position angle.

$$\begin{aligned} \Delta\mathrm{PA} &= |\mathrm{PA}_1 - \mathrm{PA}_2| \qquad (|\mathrm{PA}_1 - \mathrm{PA}_2| \leq 90^\circ) \\ \Delta\mathrm{PA} &= 180 - |\mathrm{PA}_1 - \mathrm{PA}_2| \qquad (|\mathrm{PA}_1 - \mathrm{PA}_2| > 90^\circ) \\ 0^\circ &\leq \Delta\mathrm{PA} \leq 90^\circ \end{aligned} \tag{1}$$

https://doi.org/10.1017/S1743921323004039 Published online by Cambridge University Press

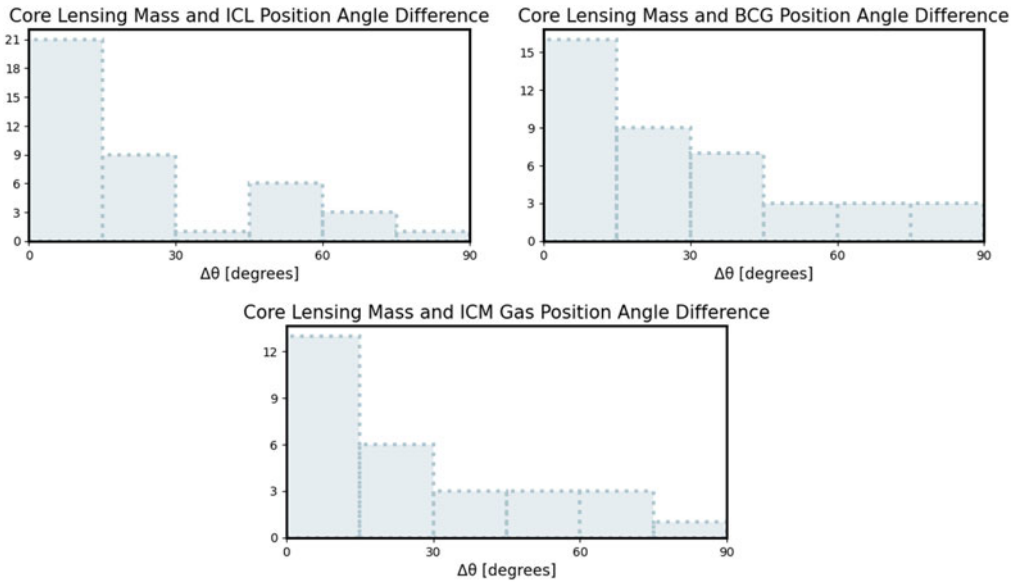

Figure 2. The difference in position angle of the major axis between the core lensing mass and the three other distributions (from top to bottom: ICL, BCG, and ICM Gas)

Generally, we measure small position angle differences which implies that cluster orientation is consistent over a large spatial scale (from a few tens of kpc up to ∼1Mpc). This behavior is consistent with previous studies (e.g. Donahue et al. 2016).

However, we still measure multiple large deviations from the expected alignment (ΔPA$> 30°$). The smaller number of deviations between the core lensing mass and ICL suggest that the ICL may be a more viable proxy for the shape and orientation of the dark matter halo distribution since it is gravitationally bound to the core halo as opposed to any specific galaxy member (Niederste-Ostholt et al. 2010; Hashimoto et al. 2014; Donahue et al. 2016).

3.2. *Ellipticities*

Figure 3 compares the ellipticity measurements of the different components of our objects. We use the definition of ellipticity analogous to the flattening parameter defined by $e = 1 - b/a$, where a and b are the semi-major axis and semi-minor axis respectively.

From the top-left panel, we see that, despite some scatter, the dark matter and stellar distribution characterized by the ICL trace out the same shape as predicted by Montes and Trujillo (2018). The bottom 2 panels reveal that the ICM is generally rounder than the dark matter and ICL which reflects the effects of hydrodynamical physics in the ICM (Markevitch and Vikhlinin 2007). In the top-right panel, we see the BCG is circularized due to dynamical friction effects as a consequence of high stellar density (Arena and Bertin 2007).

3.3. *Centroids*

From figure 4, we are able to gather an understanding of the centroid difference of the different components of our galaxy clusters when compared to one another. When

https://doi.org/10.1017/S1743921323004039 Published online by Cambridge University Press

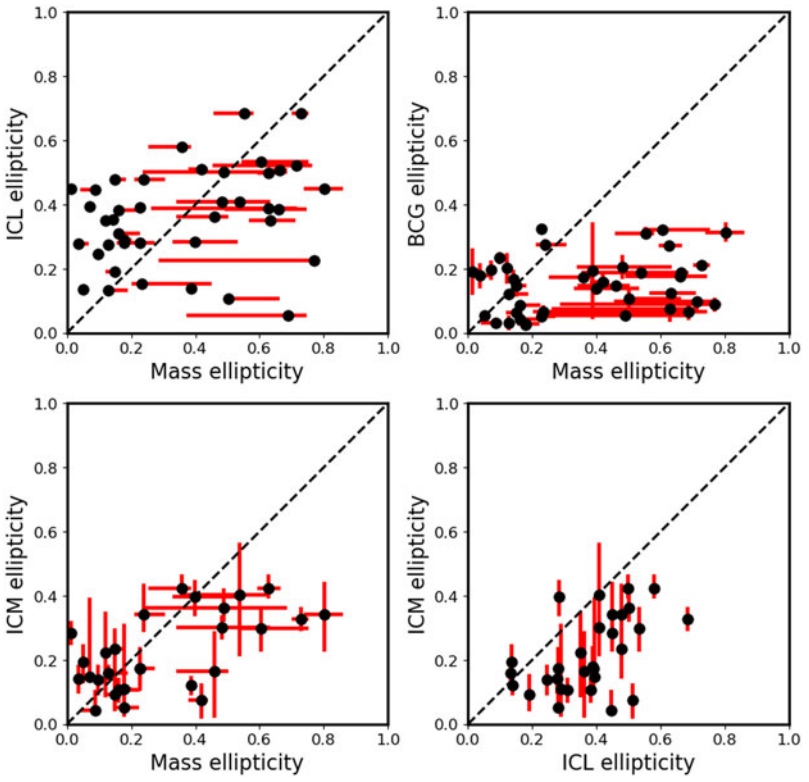

Figure 3. The ellipticity comparisons of various distributions (top-left: core lensing mass and ICL, top-right: core lensing mass and BCG, bottom-left: core lensing mass and ICM, bottom-right: ICL and ICM)

calculating the difference in centroid, we use the difference in projected radius as defined by $\Delta R = |r_1 - r_2|$ in units of kpc.

As expected, we measure small deviations in centroid for the ICL and BCG when compared to the core lensing mass. This implies that generally the BCG and ICL lie close to the center of the dark matter gravitational potential and that typically their mutual alignments coincide. The ICL is slightly more aligned with the core lensing mass distribution centroid than the BCG. This is because the BCG experiences a greater residual wobble around the dark matter gravitational center than the ICL.

Even after excluding double cored systems undergoing obvious major mergers, we still see that the ICM Gas is displaced to a much larger projected radius than the ICL or BCG. This is likely due to the fact that the ICM Gas "sloshes" as a consequence of major merger activity in the cluster's past (Markevitch et al. 2001; Churazov et al. 2003; Johnson et al. 2012; Harvey et al. 2017). The sloshing behavior is found to persist in cases where the BCG and ICL distributions have relaxed back to the core lensing mass centroid since these oscillations are damped on a much longer time scale due to hydrodynamical processes that only affect the ICM (Markevitch and Vikhlinin 2007).

https://doi.org/10.1017/S1743921323004039 Published online by Cambridge University Press

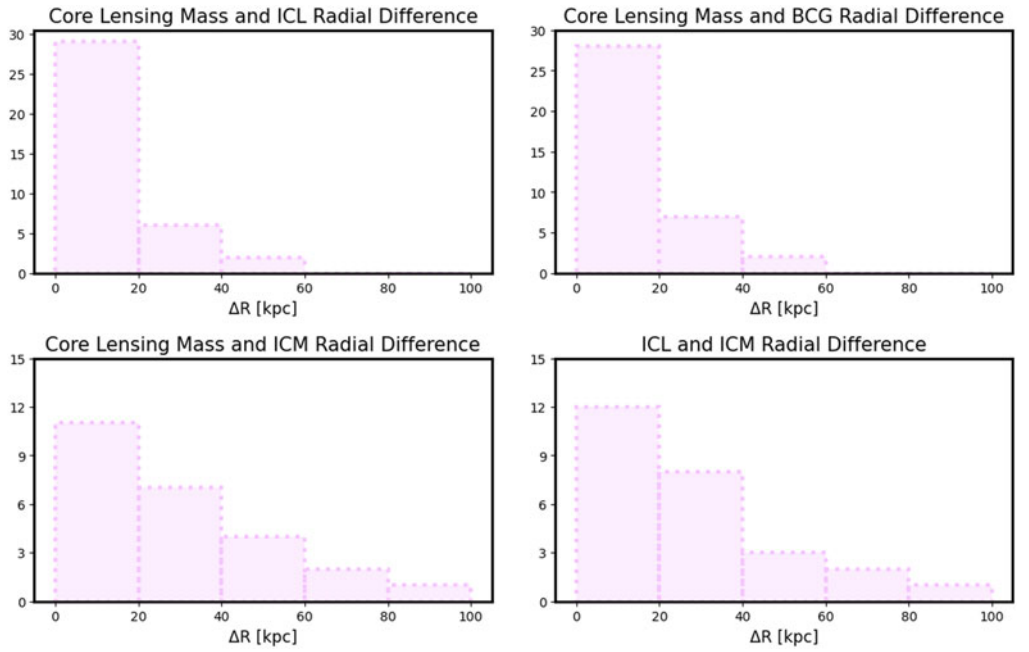

Figure 4. The centroid comparisons of various distributions (top-left: core lensing mass and ICL, top-right: core lensing mass and BCG, bottom-left: core lensing mass and ICM, bottom-right: ICL and ICM). We exclude doubly cored systems with extrememly large deviations

References

Arena, S. E. & Bertin, G. 2007, Slow evolution of elliptical galaxies induced by dynamical friction. III. Role of density concentration and pressure anisotropy. *AAP*, 463(3), 921–935.

Beers, T. & Geller, M. 1983, The environment of d and cd galaxies. *ApJ*, 274, 491.

Biernacka, M., Panko, E., Bajan, K., Godłowski, W., & Flin, P. 2015, The alignment of galaxy structures. *ApJ*, 813(1), 20.

Binggeli, B. 1982, The shape and orientation of clusters of galaxies. *PASP*, 107, 338.

Churazov, E., Forman, W., Jones, C., & Böhringer, H. 2003, Xmm-newton observations of the perseus cluster. i. the temperature and surface brightness structure. *ApJ*, 590(1), 225.

Contini, E., Chen, H. Z., & Gu, Q. 2022, The transition region between brightest cluster galaxies and intracluster light in galaxy groups and clusters. *ApJ*, 928, 99.

De Propris, R., West, M. J., Andrade-Santos, F., Ragone-Figueroa, C., Rasia, E., Forman, W., Jones, C., Kipper, R., Borgani, S., Lambas, D. G., Romashkova, E. A., & Patra, K. C. 2021, Brightest cluster galaxies: the centre can(not?) hold. *MNRAS*, 500(1), 310–318.

Donahue, M., Ettori, S., Rasia, E., Sayers, J., Zitrin, A., Meneghetti, M., Voit, G. M., Golwala, S., Czakon, N., Yepes, G., Baldi, A., Koekemoer, A., & Postman, M. 2016, The morphologies and alignments of gas, mass, and the central galaxies of clash clusters of galaxies. *ApJ*, 819(1), 36.

Harvey, D., Courbin, F., Kneib, J. P., & McCarthy, I. G. 2017, A detection of wobbling brightest cluster galaxies within massive galaxy clusters. *MNRAS*, 472(2), 1972–1980.

Hashimoto, Y., Henry, J. P., & Boehringer, H. 2008, Alignment of galaxies and clusters. *MNRAS*, 390(4), 1562–1568.

Hashimoto, Y., Henry, J. P., & Boehringer, H. 2014, Multiwavelength investigations of co-evolution of bright cluster galaxies and their host clusters. *MNRAS*, 440(1), 588–600.

Hikage, C., Mandelbaum, R., Takada, M., & Spergel, D. N. 2013, Where are the Luminous Red Galaxies (LRGs)? Using correlation measurements and lensing to relate LRGs to dark matter haloes. *MNRAS*, 435(3), 2345–2370.

https://doi.org/10.1017/S1743921323004039 Published online by Cambridge University Press

Hoshino, H., Leauthaud, A., Lackner, C., Hikage, C., Rozo, E., Rykoff, E., Mandelbaum, R., More, S., More, A., Saito, S., & Vulcani, B. 2015, Luminous red galaxies in clusters: central occupation, spatial distributions and miscentring. *MNRAS*, 452(1), 998–1013.

Johnson, R. E., Zuhone, J., Jones, C., Forman, W. R., & Markevitch, M. 2012, Sloshing gas in the core of the most luminous galaxy cluster rxj1347.5-1145. *MNRAS*, 751(2), 95.

Jullo, E., Kneib, J.-P., Limousin, M., Elíasdóttir, Á., Marshall, P. J., & Verdugo, T. 2007, A bayesian approach to strong lensing modelling of galaxy clusters. *New J. Phys.*, 9(12), 447.

Kim, S. Y., Peter, A. H. G., & Wittman, D. 2017, In the wake of dark giants: new signatures of dark matter self-interactions in equal-mass mergers of galaxy clusters. *MNRAS*, 469(2), 1414–1444.

Lange, J. U., van den Bosch, F. C., Hearin, A., Campbell, D., Zentner, A. R., Villarreal, A. S., & Mao, Y.-Y. 2018, Brightest galaxies as halo centre tracers in SDSS DR7. *MNRAS*, 473(2), 2830–2851.

Lauer, T. R., Postman, M., Strauss, M. A., Graves, G. J., & Chisari, N. E. 2014, Brightest cluster galaxies at the present epoch. *ApJ*, 797(2), 82.

Lopes, P. A. A., Trevisan, M., Laganá, T. F., Durret, F., Ribeiro, A. L. B., & Rembold, S. B. 2018, Optical substructure and BCG offsets of Sunyaev–Zel'dovich and X-ray-selected galaxy clusters. *MNRAS*, 478(4), 5473–5490.

Markevitch, M. & Vikhlinin, A. 2007, Shocks and cold fronts in galaxy clusters. *Phys. Rep.*, 443(1), 1–53.

Markevitch, M., Vikhlinin, A., & Mazzotta, P. 2001, Nonhydrostatic gas in the core of the relaxed galaxy cluster a1795. *ApJ*, 562(2), L153.

Martel, H., Robichaud, F., & Barai, P. 2014, Major cluster mergers and the location of the brightest cluster galaxy. *ApJ*, 786(2), 79.

Montes, M. & Trujillo, I. 2018, Intracluster light: a luminous tracer for dark matter in clusters of galaxies. *MNRAS*, 482(2), 2838–2851.

Niederste-Ostholt, M., Strauss, M. A., Dong, F., Koester, B. P., & McKay, T. A. 2010, Alignment of brightest cluster galaxies with their host clusters. *MNRAS*, 405(3), 2023–2036.

Oliva-Altamirano, P., Brough, S., Lidman, C., Couch, W. J., Hopkins, A. M., Colless, M., Taylor, E., Robotham, A. S. G., Gunawardhana, M. L. P., Ponman, T., Baldry, I., Bauer, A. E., Bland-Hawthorn, J., Cluver, M., Cameron, E., Conselice, C. J., Driver, S., Edge, A. C., Graham, A. W., van Kampen, E., Lara-López, M. A., Liske, J., López-Sánchez, A. R., Loveday, J., Mahajan, S., Peacock, J., Phillipps, S., Pimbblet, K. A., & Sharp, R. G. 2014, Galaxy And Mass Assembly (GAMA): testing galaxy formation models through the most massive galaxies in the Universe. *MNRAS*, 440(1), 762–775.

Rossetti, M., Gastaldello, F., Ferioli, G., Bersanelli, M., De Grandi, S., Eckert, D., Ghizzardi, S., Maino, D., & Molendi, S. 2016, Measuring the dynamical state of Planck SZ-selected clusters: X-ray peak – BCG offset. *MNRAS*, 457(4), 4515–4524.

Sanderson, A. J. R., Edge, A. C., & Smith, G. P. 2009, LoCuSS: the connection between brightest cluster galaxy activity, gas cooling and dynamical disturbance of X-ray cluster cores. *MNRAS*, 398(4), 1698–1705.

Sastry, G. N. 1968, Clusters associated with supergiant galaxies. *PASP*, 80(474), 252.

Sharon, K., Bayliss, M. B., Dahle, H., Dunham, S. J., Florian, M. K., Gladders, M. D., Johnson, T. L., Mahler, G., Paterno-Mahler, R., Rigby, J. R., Whitaker, K. E., Akhshik, M., Koester, B. P., Murray, K., González, J. D. R., & Wuyts, E. 2020, Strong lens models for 37 clusters of galaxies from the sdss giant arcs survey*. *ApJS*, 247(1), 12.

Sharon, K., Cerny, C., Rigby, J. R., Florian, M. K., Bayliss, M. B., Dahle, H., Gladders, M. D., & Mahler, G. 2022,a HST-Based Lens Model of SDSS J1226+2152, in Preparation for JWST-ERS TEMPLATES. *arXiv e-prints*, arXiv:2207.05709.

Sharon, K., Mahler, G., Rivera-Thorsen, T. E., Dahle, H., Gladders, M. D., Bayliss, M. B., Florian, M. K., Kim, K. J., Khullar, G., Mainali, R., Napier, K. A., Navarre, A., Rigby, J. R., Remolina González, J. D., & Sharma, S. 2022,b The Cosmic Telescope That Lenses the Sunburst Arc, PSZ1 G311.65-18.48: Strong Gravitational Lensing Model and Source Plane Analysis. *ApJ*, 941b(2), 203.

Skibba, R. A., van den Bosch, F. C., Yang, X., More, S., Mo, H., & Fontanot, F. 2011, Are brightest halo galaxies central galaxies? *MNRAS*, 410(1), 417–431.

Van Den Bosch, F. C., Weinmann, S. M., Yang, X., Mo, H. J., Li, C., & Jing, Y. P. 2005, The phase-space parameters of the brightest halo galaxies. *MNRAS*, 361(4), 1203–1215.

Wang, L., Yang, X., Shen, S., Mo, H. J., van den Bosch, F. C., Luo, W., Wang, Y., Lau, E. T., Wang, Q. D., Kang, X., & Li, R. 2014, Measuring the X-ray luminosities of SDSS DR7 clusters from ROSAT All Sky Survey. *MNRAS*, 439(1), 611–622.

Wang, P., Luo, Y., Kang, X., Libeskind, N. I., Wang, L., Zhang, Y., Tempel, E., & Guo, Q. 2018, Alignment between satellite and central galaxies in the sdss dr7: Dependence on large-scale environment. *ApJ*, 859(2), 115.

Wittman, D., Foote, D., & Golovich, N. 2019, Brightest cluster galaxy alignments in merging clusters. *ApJ*, 874(1), 84.

Zenteno, A., Hernández-Lang, D., Klein, M., Vergara Cervantes, C., Hollowood, D. L., Bhargava, S., Palmese, A., Strazzullo, V., Romer, A. K., Mohr, J. J., Jeltema, T., Saro, A., Lidman, C., Gruen, D., Ojeda, V., Katzenberger, A., Aguena, M., Allam, S., Avila, S., Bayliss, M., Bertin, E., Brooks, D., Buckley-Geer, E., Burke, D. L., Capasso, R., Carnero Rosell, A., Carrasco Kind, M., Carretero, J., Castander, F. J., Costanzi, M., da Costa, L. N., De Vicente, J., Desai, S., Diehl, H. T., Doel, P., Eifler, T. F., Evrard, A. E., Flaugher, B., Floyd, B., Fosalba, P., Frieman, J., García-Bellido, J., Gerdes, D. W., Gonzalez, J. R., Gruendl, R. A., Gschwend, J., Gutierrez, G., Hartley, W. G., Hinton, S. R., Honscheid, K., James, D. J., Kuehn, K., Lahav, O., Lima, M., McDonald, M., Maia, M. A. G., March, M., Melchior, P., Menanteau, F., Miquel, R., Ogando, R. L. C., Paz-Chinchón, F., Plazas, A. A., Roodman, A., Rykoff, E. S., Sanchez, E., Scarpine, V., Schubnell, M., Serrano, S., Sevilla-Noarbe, I., Smith, M., Soares-Santos, M., Suchyta, E., Swanson, M. E. C., Tarle, G., Thomas, D., Varga, T. N., Walker, A. R., Wilkinson, R. D., & Collaboration), D. 2020, A joint SZ–X-ray–optical analysis of the dynamical state of 288 massive galaxy clusters. *MNRAS*, 495(1), 705–725.

Zitrin, A., Bartelmann, M., Umetsu, K., Oguri, M., & Broadhurst, T. 2012, Miscentring in galaxy clusters: dark matter to brightest cluster galaxy offsets in 10000 Sloan Digital Sky Survey clusters. *MNRAS*, 426(4), 2944–2956.